

# STABILIZER-FREE POLYGONAL AND POLYHEDRAL VIRTUAL ELEMENTS

YANPING LIN, MO MU, AND SHANGYOU ZHANG

ABSTRACT. Stabilizer-free  $P_k$  virtual elements are constructed on polygonal and polyhedral meshes. Here the interpolating space is the space of continuous  $P_k$  polynomials on a triangular-subdivision of each polygon, or a tetrahedral-subdivision of each polyhedron. With such an accurate and proper interpolation, the stabilizer of the virtual elements is eliminated while the system is kept positive-definite. We show that the stabilizer-free virtual elements converge at the optimal order in 2D and 3D. Numerical examples are computed, validating the theory.

## 1. INTRODUCTION

The virtual element method is proposed and studied in [4, 5, 9, 10, 11, 12, 13, 15, 16, 20, 21, 22]. In this work, we construct stabilizer-free  $P_k$  virtual elements on polygonal and polyhedral meshes.

We consider the Poisson equation,

$$(1.1) \quad \begin{aligned} -\Delta u &= f && \text{in } \Omega, \\ u &= 0 && \text{on } \partial\Omega, \end{aligned}$$

where  $\Omega \subset \mathbb{R}^d$  is a bounded polygonal or polyhedral domain and  $f \in L^2(\Omega)$ . The variation form reads: Find  $u \in H_0^1(\Omega)$  such that

$$(1.2) \quad (\nabla u, \nabla v) = (f, v) \quad \forall v \in H_0^1(\Omega),$$

where  $(\cdot, \cdot)$  is the  $L^2$  inner product on  $\Omega$  and we have  $|v|_1^2 = (\nabla v, \nabla v)$ .

Let  $\mathcal{T}_h = \{K\}$  be a quasi-uniform polygonal or polyhedral mesh on  $\Omega$  with  $h$  as the maximum size of the polygons or polyhedrons  $K$ . Let  $\mathcal{E}_h$  denote the set of edges  $e$  in  $\mathcal{T}_h$ . In 3D, let  $\mathcal{F}_h$  be the set of all face-polygons  $F$  in

---

2010 *Mathematics Subject Classification.* 65N15, 65N30.

*Key words and phrases.* virtual element, stabilizer free, elliptic equation, Hsieh-Clough-Tocher macro-triangle, triangular mesh.

Yanping Lin is supported in part by HKSAR GRF 15302922 and polyu-CAS joint Lab. Mo Mu is supported in part by Hong Kong RGC CERG HKUST16301218.

$\mathcal{T}_h$ . For  $k \geq 1$ , the virtual element space is defined as

$$(1.3) \quad \begin{aligned} \tilde{V}_h &= \{v \in H_0^1(\Omega) : \tilde{v} \in \mathbb{B}_k(\mathcal{E}_h), \Delta \tilde{v}|_K \in P_{k-2}(K)\} \text{ in 2D, or as} \\ \tilde{V}_h &= \{v \in H_0^1(\Omega) : \tilde{v} \in \mathbb{B}_k(\mathcal{E}_h); \Delta_F \tilde{v}|_F \in P_{k-2}(F), F \in \mathcal{F}_h; \\ &\quad \Delta \tilde{v}|_K \in P_{k-2}(K)\} \end{aligned}$$

in 3D, where  $P_{-1} = \{0\}$ ,  $\mathbb{B}_k(\mathcal{E}_h) = \{v \in C^0(\mathcal{E}_h) : v|_e \in P_k(e) \forall e \subset \mathcal{E}_h\}$ , and  $\Delta_F$  is the 2D Laplacian on the flat polygon  $F$ . In computation, the interpolated virtual finite element space on  $\mathcal{T}_h$  is defined by

$$(1.4) \quad V_h = \{v_h = \Pi_h^\nabla \tilde{v} : v_h|_K \in \mathbb{V}_k(K), K \in \mathcal{T}_h; \tilde{v} \in \tilde{V}_h\},$$

where  $\mathbb{V}_k(K) = P_k(K)$  for the standard virtual elements (and to be defined below in (2.1) for the new virtual element method), and  $v_h = \Pi_h^\nabla \tilde{v}$  is the local  $H^1$ -projection:

$$\begin{cases} (\nabla(v_h - \tilde{v}), \nabla w_h)_K = 0 & \forall w_h = \Pi_h^\nabla \tilde{w} \in \mathbb{V}_k(K), \\ \langle v_h - \tilde{v}, w_h \rangle_{\partial K} = 0 & \forall w_h \in P_k(K). \end{cases}$$

The stabilizer-free virtual element equation reads: Find  $u_h = \Pi_h^\nabla \tilde{u} \in V_h$  such that

$$(1.5) \quad (\nabla u_h, \nabla v_h)_h = (f, v_h) \quad \forall \tilde{v} \in \tilde{V}_h, v_h = \Pi_h^\nabla \tilde{v},$$

where  $(\nabla u_h, \nabla v_h)_h = \sum_{K \in \mathcal{T}_h} (\nabla u_h, \nabla v_h)_K$ . In 3D, to find the value of  $\tilde{v}$  inside a face-polygon, we use the moments  $\int_F \tilde{v}_h p_{k-2} dS$  instead of the surface Laplacian values  $\Delta_F \tilde{v}_h \in P_{k-2}(F)$ , as the latter uniquely determines  $\tilde{v}_h$  and consequently uniquely determines the  $P_{k-2}$  moments of  $\tilde{v}_h$  on  $F$ .

Because the dimension of  $V_h$  is less than that of  $\tilde{V}_h$  (equal only when  $k = 1$  on triangular and tetrahedral meshes), the bilinear form in (1.5) is not positive-definite and the equation does not have a unique solution. Thus a discrete stabilizer must be added to the equation (1.5) if the interpolation space  $\mathbb{V}_k(K)$  is defined to be  $P_k(K)$ .

With a stabilizer, many degrees of freedom do not fully contribute their approximation power as they are averaged into a smaller dimensional vector space. To be a stabilizer free virtual element, the interpolation space must have at least no less degrees of freedom on each element. But raising the polynomial degree of  $\mathbb{V}_k(K)$  in (1.4) does not work. It works only for  $P_1$  virtual elements in 2D with special treatment, cf. [6, 7], where  $\mathbb{V}_k(K) = P_{k+l(n)}(K)$  and  $n$  is the number of edges of  $K$ , in the virtual element space (1.4). Another stabilizer-free method for  $k = 1$  is proposed in [8] that  $\mathbb{V}_k(K) = P_k(K) \cup H_l(K)$ , where  $H_l(K)$  is the set of 2D harmonic polynomials

of degree  $l$  or less, and  $l$  depends on the number of edges of  $K$ . This is an excellent idea because the  $H_l$  harmonic polynomials may help to gather all boundary edge values while not destroying the gradient approximation, as harmonic polynomials have vanishing Laplacian. The same idea has been implemented in some other finite elements [1, 28, 29]. But the method of [8] is also for 2D  $P_1$  polygonal elements, as it is shown numerically not working for  $k > 3$  in [35].

We propose to use macro-triangles or macro-tetrahedrons  $C^0$ - $P_k$  spaces as the interpolation space  $\mathbb{V}_k(K)$  in (1.4). This method was first used in [35] for  $P_k$  triangular virtual elements only. In [35], each triangle  $K$  is split into three triangles by connecting its barycenter with the three vertices.  $K$  is called a Hsieh-Clough-Tocher macro-triangle [14, 29, 34, 58, 59]. In this work, we extend the method to polygonal and polyhedral virtual elements. It turns out that the triangular virtual element would be the most complicated case, as we have to introduce a new point in the subdivision in order to get a sufficiently large dimensional vector space. For most polygons and polyhedrons we can subdivide them into triangles and tetrahedrons respectively without adding any new point, when we have enough face-edge and face-polygon degrees of freedom.

A different interpolation space  $\mathbb{V}_k$  changes the quadrature rule for computing  $(\nabla u_h, \nabla v_h) = (\nabla \Pi_h^\nabla \tilde{u}, \nabla \Pi_h^\nabla \tilde{v})$ . Such an accurate local interpolation does not increase the computational cost, once the local stiffness matrix is generated. On the other side, eliminating the stabilizer may reduce computational cost, and may improve the condition number of the resulting linear system. More importantly, a stabilizer-free method may utilize fully every degree of freedom in the discrete approximation. Thus stabilizer-free methods may result in superconvergence.

The stabilizer is eliminated in the weak Galerkin finite element method [2, 18, 19, 23, 30, 31, 38, 39, 40, 43, 44, 45]. It is also eliminated in the  $H(\text{div})$  finite element method [24, 42, 47]. The stabilizer-free  $C^0$  or  $C^{-1}$  nonconforming finite elements are constructed for the biharmonic equation [41, 49, 50]. We have stabilizer-free discontinuous Galerkin finite element methods [17, 26, 36, 37, 41]. Without a stabilizer, two-order superconvergent weak Galerkin finite elements are found in [3, 32, 33, 48, 54, 57]. Also two-order superconvergent stabilizer-free discontinuous Galerkin finite elements are constructed in [51, 52, 55] for second order elliptic equations. One or

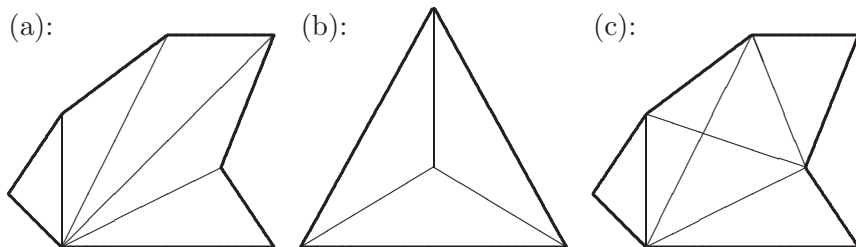


FIGURE 1. (a) A polygon is subdivided without any new point. (b) A triangle must be subdivided with one new point. (c) A polygon is subdivided with one new point.

two-order superconvergent weak Galerkin finite elements are found for the Stokes equations in [25, 46, 53]. Four-order superconvergent weak Galerkin finite elements [56] and four-order superconvergent discontinuous Galerkin finite elements [52, 57] are all stabilizer-free, for the biharmonic equation. For example, a  $P_3$  discontinuous finite element solution is as accurate as a  $C^1$ - $P_7$  finite element solution in solving a 2D biharmonic equation.

In this paper, we show that with the macro-triangle/tetrahedron interpolation, the stabilizer-free virtual element equation (1.5) has a unique and quasi-optimal solution. Numerical examples on the new stabilizer-free virtual elements are computed, verifying the theory.

## 2. THE 2D INTERPOLATION

We define in this section the 2D macro-triangle interpolation space and show that the stabilizer-free virtual element equation has a unique solution.

Let  $K$  be a 2D polygon. The only requirement is that  $K$  is subdivided into more than one tetrahedron. If  $K$  has only three sides, i.e.,  $K$  is a triangle, we add a barycenter point to the triangle, shown as in the Figure 1(b) macro triangle on  $K$ . If  $K$  is a polygon of four sides or more, we usually can connect some vertices of  $K$  to subdivide  $K$  into a macro-triangle polygon, cf. Figure 1(a). If needed, we can add one or two inner points to subdivide  $K$ , cf. Figure 1(c), where we intentionally add a new point for the purpose of illustration. With the subdivision  $K = \cup_{T_i \subset K} T_i$ , we define the interpolation space as, for  $k \geq 1$ ,

$$(2.1) \quad \mathbb{V}_k(K) = \{v_h \in C^0(K) : v_h|_{T_i} \in P_k(T_i), T_i \subset K\}.$$

One can easily count the internal degrees of freedom of  $\mathbb{V}_k(K)$  to get

$$\dim(\mathbb{V}_k \cap H_0^1(K)) > \dim P_{k-2}(K).$$

The interpolation operator is defined to be the local  $H^1$ -projection, i.e.,  $v_h = \Pi_h^\nabla \tilde{v} \in \mathbb{V}_k$  such that  $v_h|_{\partial K} = \tilde{v}$  and

$$(2.2) \quad (\nabla(v_h - \tilde{v}), \nabla w_h) = 0 \quad \forall w_h \in \mathbb{V}_k(K).$$

**Lemma 2.1.** *The interpolation operator  $\Pi_h^\nabla$  is well defined in (2.2) and it preserves  $P_k$  polynomials,*

$$(2.3) \quad \Pi_h^\nabla \tilde{v} = \tilde{v} \quad \text{if } \tilde{v} \in P_k(K).$$

*Proof.* Because  $\tilde{v}|_{\partial K} \in \mathbb{B}_k(\mathcal{E}_h)$ ,  $v_h$  can assume the boundary condition  $v_h = \tilde{v}$  exactly on  $\partial K$ . The linear system of equations in (2.2) is a finite dimensional square system. The existence is implied by the uniqueness. To show the uniqueness, we let  $\tilde{v} = 0$  in (2.2). Letting  $w_h = v_h$  in (2.2), we get

$$\nabla v_h = \mathbf{0} \quad \text{on } K.$$

Thus  $v_h = c$  is a constant on  $K$ . As  $v_h$  is continuous on edges,  $v_h = c$  is a global constant on the whole domain. By the boundary condition, we get  $0 = \tilde{v}|_{\partial\Omega} = v_h|_{\partial\Omega} = c$ . Hence  $v_h = 0$  and (2.2) has a unique solution.

If  $\tilde{v} \in P_k(K) \subset \mathbb{V}_k(K)$ , defined in (1.4), then the solution of (2.2) says, letting  $w_h = v_h - \tilde{v}$ ,

$$\nabla(v_h - \tilde{v}) = \mathbf{0}.$$

Thus  $v_h - \tilde{v}$  is a global constant which must be zero as it vanishes at all  $\partial K$ . (2.3) is proved.  $\square$

**Lemma 2.2.** *The stabilizer-free virtual element equation (1.5) has a unique solution, where the interpolation  $\Pi_h^\nabla$  is defined in (2.2).*

*Proof.* As both  $\tilde{u}, \tilde{v} \in \tilde{V}_h$ , (1.5) is a finite square system of linear equations. The uniqueness of solution implies the existence. To show the uniqueness, we let  $f = 0$  and  $\tilde{v} = \tilde{u}$  in (1.5). It follows that

$$|\Pi_h^\nabla \tilde{u}|_{1,h} = 0.$$

Thus  $\Pi_h^\nabla \tilde{u} = c$  is constant on each  $K$ . But  $\Pi_h^\nabla \tilde{u}$  is continuous on the whole domain. By the boundary condition, we get  $0 = \Pi_h^\nabla \tilde{u}|_{\partial\Omega} = c$ . That is,

$$(2.4) \quad \Pi_h^\nabla \tilde{u} = 0 \quad \text{and} \quad \tilde{u}|_{\partial K} = \Pi_h^\nabla \tilde{u} = 0.$$

For  $k = 1$ ,  $\tilde{u}$  has no internal degree of freedom, and the lemma is proved by (2.4),

$$\tilde{u} = 0, \quad \text{if } k = 1.$$

For  $k \geq 2$ , let

$$(2.5) \quad b_K = \sum_{i \in \mathcal{N}_2} \phi_i \in H_0^1(K) \cap \mathbb{V}_k(K),$$

where  $\mathcal{N}_2$  is the set of all internal mid-edge points of  $\{T_i\}$ ,  $K = \cup T_i$ , and  $\phi_i$  is the  $P_2$  Lagrange nodal basis at node  $i$ . Then  $b_K > 0$  inside polygon  $K$  if it does not have any added internal point, cf. Figure 1. Otherwise,  $b_K > 0$  inside  $K$  except at one or two internal points where  $b_K = 0$ .

On one polygon  $K$ , by (2.2), (2.4) and integration by parts, we have

$$(2.6) \quad (-\Delta \tilde{u}, w_h) = (\nabla \tilde{u}, \nabla w_h) = 0 \quad \forall w_h \in H_0^1(K) \cap \mathbb{V}_k(K).$$

By the space  $\tilde{V}_h$  definition (1.3), we denote

$$(2.7) \quad p_{k-2} = -\Delta \tilde{u} \in P_{k-2}(K).$$

Let the  $w_h$  in (2.6) be

$$(2.8) \quad w_h = p_{k-2} b_K \in H_0^1(K) \cap \mathbb{V}_k(K),$$

where the positive  $P_2$  bubble  $b_K$  is defined in (2.5). With the  $w_h$  in (2.8), we get from (2.6) and (2.7) that

$$\int_K p_{k-2}^2 b_K d\mathbf{x} = 0.$$

As  $b_K > 0$  inside  $K$  (other than 1 or 2 possibly internal points), it follows that

$$p_{k-2}^2 = 0 \quad \text{and} \quad p_{k-2} = 0 \quad \text{on } K.$$

By (2.4) and (2.7),  $\Delta \tilde{u} = 0$  in  $K$  and  $\tilde{u} = 0$  on  $\partial K$ . Thus, by the unique solution of the Laplace equation,  $\tilde{u} = 0$ . The lemma is proved.  $\square$

### 3. THE 3D INTERPOLATION

We define in this section the 3D macro-tetrahedron interpolation space and show that the stabilizer-free virtual element equation has a unique solution when using the interpolation.

Let  $K$  be a 3D polyhedron. The first requirement is that each face-polygon  $F$  must be subdivided into more than one triangle. The subdivision

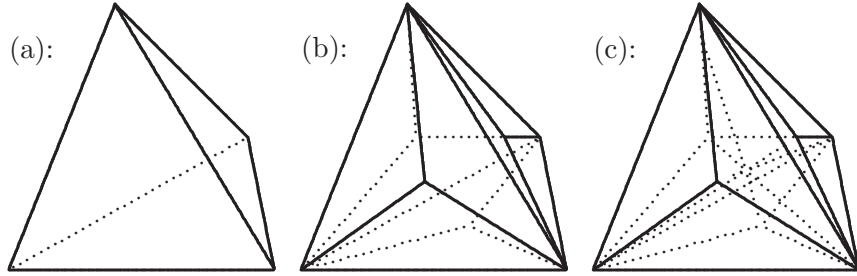


FIGURE 2. (a) A tetrahedron  $K$ . (b) By adding a barycenter point to each face-triangle, the face triangles of  $K$  are subdivided into twelve triangles. (c) By adding one barycenter point of  $K$ , the tetrahedron  $K$  is subdivided into twelve tetrahedrons.

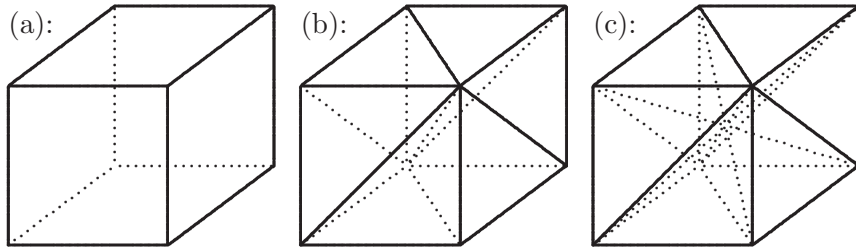


FIGURE 3. (a) A polyhedron  $K$ . (b) A polyhedron is subdivided into six tetrahedrons without adding any point. (c) A polyhedron is subdivided into twelve tetrahedrons with one new point and without adding any face point.

of polygons is defined in the last section. For example, if a face polygon  $F$  has only three sides, i.e.,  $F$  is a triangle, we must add a barycenter point to subdivide it into three triangles, cf. Figure 2(b). However if a face polygon has more than three edges, we usually can subdivide it into triangles easily, cf. Figure 3(b). After each face polygon is subdivided into more than one triangle, the next requirement in subdividing  $K$  is that every resulting tetrahedron has at least two face-triangles inside  $K$ .

For example, after cutting each face-triangle of a tetrahedron  $K$  into three triangles, we add one more internal point to cut  $K$  into twelve tetrahedrons, cf. Figure 2(c).

For example, for the polyhedron  $K$  of a cube in Figure 3(a), we cut each face-polygon into two triangles without adding any point, and we cut  $K$  into six tetrahedrons without adding any internal point, cf. Figure 3(b).

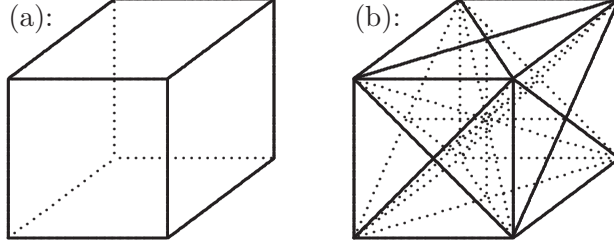


FIGURE 4. (a) A polyhedron  $K$ . (b) A polyhedron is subdivided into twenty four tetrahedrons with one new point each face-polygon and one internal point.

For example, for the polyhedron  $K$  of a cube in Figure 3(a), we can also subdivide it by cutting each face-polygon into two triangles without adding any point, and cutting  $K$  into twelve tetrahedrons with one internal point, cf. Figure 3(c).

For example, for the polyhedron  $K$  of a cube in Figure 4(a), we can also subdivide it by cutting each face-polygon into four triangles with one added point on each face-polygon, and cutting  $K$  into twenty four tetrahedrons with one additional point inside  $K$ , cf. Figure 4(b).

In the analysis, we assume the same face-polygon subdivision on the two polyhedrons sharing the polygon. In the computation, the subdivisions of a shared polygon on the two sides can be different as the interpolation and the computation on the two polyhedrons are independent of each other. We can extend the theory easily to cover the case that different triangulations on a face-polygon of two polyhedrons, as both interpolations are the 2D  $H^1$  projection of same  $P_{k-2}$  moments.

With a proper tetrahedral subdivision of  $K = \cup_{T_i \subset K} T_i$ , cf. Figures 2–4, we define the interpolation space on  $K$  as, for  $k \geq 1$ , in (2.1), again in 3D.

The interpolation operator is defined by two steps. On each face polygon  $F \in \mathcal{F}_h$ , we solve an  $H^1$  projection problem that  $v_h|_F = \Pi_h^\nabla \tilde{v} \in \mathbb{V}_k(F)$  (the restriction of  $\mathbb{V}_k(K)$  on  $F$ ) satisfying

$$(3.1) \quad \begin{aligned} (\nabla_F(v_h|_F - \tilde{v}), \nabla_F w_h) &= 0 \quad \forall w_h \in \mathbb{V}_k(F) \cap H_0^1(F), \\ v_h|_F - \tilde{v} &= 0 \quad \text{on } \partial F, \end{aligned}$$

where  $\nabla_F$  is the 2D face gradient. This way, the boundary value of  $\Pi_h^\nabla \tilde{v}$  is determined on  $\partial K$ . The interpolation in 3D is defined as the 3D local

$H^1$ -projection, i.e.,  $v_h = \Pi_h^\nabla \tilde{v} \in \mathbb{V}_k$  such that

$$(3.2) \quad \begin{aligned} (\nabla(v_h - \tilde{v}), \nabla w_h) &= 0 \quad \forall w_h \in \mathbb{V}_k(K) \cap H_0^1(K), \\ v_h - v_h|_F &= 0 \quad \text{on all } F \in \partial K, \end{aligned}$$

where  $v_h|_F$  is defined in (3.1).

**Lemma 3.1.** *The interpolation operator  $\Pi_h^\nabla$  is well defined in (3.2) and it preserves  $P_k$  polynomials,*

$$(3.3) \quad \Pi_h^\nabla \tilde{v} = \tilde{v} \quad \text{if } \tilde{v} \in P_k(K).$$

*Proof.* Because  $\tilde{v}|_{\partial F} \in \mathbb{B}_k(\mathcal{E}_h)$ ,  $v_h$  can assume the boundary condition  $v_h = \tilde{v}$  exactly on  $\partial F$ , where  $F$  is a face-polygon in the polyhedral mesh. As we have proved in Lemma 2.1,  $v_h|_F$  is well-defined in (3.1). Further by Lemma 2.1,

$$(3.4) \quad v_h|_F = p_k|_F \quad \text{if } p_k = \tilde{v} \in P_k(K).$$

The linear system of equations in (3.2) is a finite dimensional square system, after the boundary condition is enforced. The existence is implied by the uniqueness. To show the uniqueness, we let  $\tilde{v} = 0$  in (3.2). By Lemma 2.1,  $v_h|_F = 0$ . Letting  $w_h = v_h$  in (3.2), we get

$$\nabla v_h = \mathbf{0} \quad \text{on } K.$$

Thus  $v_h = c$  is one constant on all tetrahedrons of  $K$ . As  $v_h$  is continuous, by the zero boundary condition,  $v_h = 0$  and (3.2) has a unique solution.

If  $\tilde{v} = p_k \in P_k(K) \subset \mathbb{V}_k(K)$ , then (3.2) says, letting  $w_h = v_h - p_k$ ,

$$\nabla(v_h - p_k) = \mathbf{0}.$$

Thus  $v_h - p_k$  is a constant on  $K$ , which must be zero by (3.4). (3.3) is proved.  $\square$

**Lemma 3.2.** *The stabilizer-free virtual element equation (1.5) has a unique solution, where the interpolation  $\Pi_h^\nabla$  is defined in (3.2).*

*Proof.* As both  $\tilde{u}, \tilde{v} \in \tilde{V}_h$ , (1.5) is a finite square system of linear equations. We only need to show the uniqueness, by letting  $f = 0$  and  $\tilde{v} = \tilde{u}$  in (1.5). As in the 2D proof of Lemma 2.2, we have

$$|\Pi_h^\nabla \tilde{u}|_{1,h} = 0 \quad \text{and} \quad \Pi_h^\nabla \tilde{u} = 0.$$

For  $k = 1$ ,  $\tilde{u}$  has no internal degree of freedom on each face polygon  $F$ , and  $\tilde{v}|_F = \Pi_h^\nabla \tilde{u}|_F = 0$ . Further  $\tilde{u}$  has no internal degree of freedom on each polyhedron  $K$ , and  $\tilde{v}|_K = \Pi_h^\nabla \tilde{u}|_K = 0$ . The lemma is proved.

For  $k \geq 2$ , by the proof of Lemma 2.2, as each face polygon is subdivided into more than one tetrahedron, we have  $\tilde{v}|_F = \Pi_h^\nabla \tilde{u}|_F = 0$  on every face polygon  $F$ . Next, as every tetrahedron has at least two internal face triangles, we define an internal  $P_2$  bubble by

$$(3.5) \quad b_K = \sum_{i \in \mathcal{N}_2} \phi_i \in H_0^1(K) \cap \mathbb{V}_k(K),$$

where  $\mathcal{N}_2$  is the set of all internal mid-edge points of  $\{T_i\}$ ,  $K = \cup T_i$ , and  $\phi_i$  is the  $P_2$  Lagrange nodal basis at node  $i$ . As every tetrahedron has such an internal  $P_2$  node (which is the shared-edge mid-point of two internal face triangles),  $b_K > 0$  inside polyhedron  $K$  if it does not have any added internal point. Otherwise,  $b_K > 0$  inside  $K$  except at one or two internal points of  $K$  where  $b_K = 0$ .

On one polyhedron  $K$ , let

$$(3.6) \quad w_h = p_{k-2} b_K \in H_0^1(K) \cap \mathbb{V}_k(K),$$

where the positive  $P_2$  bubble  $b_K$  is defined in (3.5), and  $p_{k-2} = -\Delta \tilde{u} \in P_{k-2}(K)$ . With the integration by parts, we get from (2.6) and (3.6) that

$$\int_K p_{k-2}^2 b_K dx = - \int_K \nabla \tilde{u} \nabla w_h dx = 0.$$

As  $b_K > 0$  inside  $K$  (other than 1 or 2 possibly internal points), it follows that

$$p_{k-2}^2 = 0 \quad \text{and} \quad p_{k-2} = 0 \quad \text{on} \quad K.$$

As  $\Delta \tilde{u} = 0$  in  $K$  and  $\tilde{u} = 0$  on  $\partial K$ , by the unique solution of the Laplace equation,  $\tilde{u} = 0$ . The lemma is proved.  $\square$

#### 4. CONVERGENCE

We show that the stabilizer-free virtual element solution converges at the optimal order, in this section.

**Theorem 4.1.** *Let the solution of (1.2) be  $u \in H^{k+1} \cap H_0^1(\Omega)$ . Let the stabilizer-free virtual element solution of (1.5) be  $u_h$ . Then the discrete*

solution converges at the optimal order with the following error estimate,

$$(4.1) \quad |u - u_h|_1 \leq Ch^k |u|_{k+1}.$$

*Proof.* As  $w_h \in V_h \subset H_0^1(\Omega)$ , subtracting (1.5) from (1.2), we obtain

$$(\nabla(u - u_h), \nabla w_h) = 0 \quad \forall w_h \in V_h.$$

By the Schwarz inequality, we get that

$$\begin{aligned} |u - u_h|_1^2 &= (\nabla(u - u_h), \nabla(u - I_h u)) \\ &\leq |u - u_h|_1 |u - I_h u|_1 \leq Ch^k |u|_{k+1} |u - u_h|_1, \end{aligned}$$

where  $I_h u$  is the Scott-Zhang interpolation on subdivided triangular mesh or tetrahedral mesh, cf. [27]. The theorem is proved.  $\square$

To get the optimal order  $L^2$  error estimate, we assume a full regularity for the dual problem that the solution of

$$(4.2) \quad \begin{aligned} -\Delta w &= u - u_h \quad \text{in } \Omega, \\ w &= 0 \quad \text{on } \partial\Omega, \end{aligned}$$

satisfies

$$(4.3) \quad |w|_2 \leq C \|u - u_h\|_0.$$

**Theorem 4.2.** *Let the solution of (1.2) be  $u \in H^{k+1} \cap H_0^1(\Omega)$ . Let the stabilizer-free virtual element solution of (1.5) be  $u_h$ . Then the discrete solution converges at the optimal order with the following  $L^2$  error estimate, assuming (4.3),*

$$\|u - u_h\|_0 \leq Ch^{k+1} |u|_{k+1}.$$

*Proof.* Let  $w_h = \Pi_h^\nabla \tilde{w}$  be the virtual element solution of (4.2). By (4.2), (4.3) and (4.1), we get

$$\begin{aligned} \|u - u_h\|_0^2 &= (\nabla w, \nabla(u - u_h)) = (\nabla(w - w_h), \nabla(u - u_h)) \\ &\leq Ch |w|_2 h^k |u|_{k+1} \leq Ch^{k+1} |u|_{k+1} \|u - u_h\|_0. \end{aligned}$$

Canceling a  $\|u - u_h\|_0$  on both sides, we proved the optimal-order  $L^2$  error bound.  $\square$

## 5. NUMERICAL TEST

We solve numerically the Poisson equation (1.1) on domain  $\Omega = (0, 1) \times (0, 1)$ , where an exact solution is chosen as

$$(5.1) \quad u(x, y) = \sin(\pi x) \sin(\pi y).$$

We test the  $P_k$  ( $k = 1, 2, 3, 4, 5$ ) stabilizer-free virtual elements on pentagonal meshes shown in Figure 5.

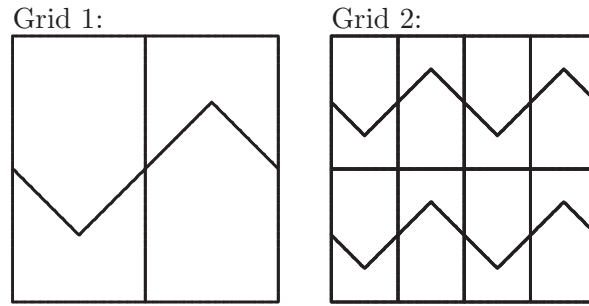


FIGURE 5. The first two levels of pentagonal meshes for the computation in Table 1.

In Table 1, we compute the  $P_1$ – $P_5$  stabilizer-free virtual elements solutions for (5.1) on the pentagonal meshes shown in Figure 5. All virtual element solutions converge at rates of the optimal order in both  $L^2$  and  $H^1$  norms.

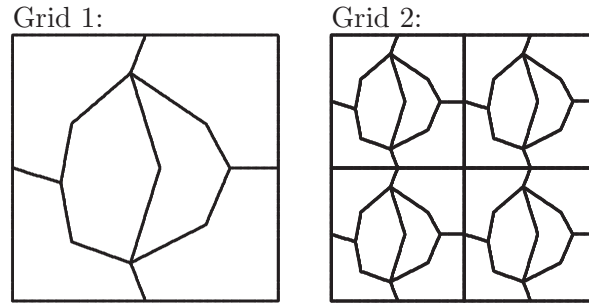


FIGURE 6. The first two levels of hexagonal grids for the computation in Table 2.

In Table 2, we compute the  $P_1$ – $P_5$  stabilizer-free virtual elements solutions for (5.1) on the hexagonal meshes shown in Figure 6. All virtual element solutions converge at rates of the optimal order in both  $L^2$  and  $H^1$  norms.

TABLE 1. The error profile for (5.1) on meshes shown in Figure 5.

Grid	$\ \Pi_h^\nabla u - u_h\ _0$	$O(h^r)$	$ \Pi_h^\nabla u - u_h _1$	$O(h^r)$
By the $P_1$ stabilizer-free virtual element.				
7	0.4462E-04	2.00	0.5834E-02	1.00
8	0.1116E-04	2.00	0.2916E-02	1.00
9	0.2789E-05	2.00	0.1458E-02	1.00
By the $P_2$ stabilizer-free virtual element.				
7	0.1930E-06	3.00	0.1131E-03	2.00
8	0.2413E-07	3.00	0.2826E-04	2.00
9	0.3016E-08	3.00	0.7066E-05	2.00
By the $P_3$ stabilizer-free virtual element.				
6	0.2486E-07	4.00	0.8973E-05	3.00
7	0.1554E-08	4.00	0.1122E-05	3.00
8	0.9716E-10	4.00	0.1402E-06	3.00
By the $P_4$ stabilizer-free virtual element.				
5	0.1051E-07	5.00	0.1977E-05	4.00
6	0.3286E-09	5.00	0.1236E-06	4.00
7	0.1027E-10	5.00	0.7724E-08	4.00
By the $P_5$ stabilizer-free virtual element.				
3	0.7591E-06	6.02	0.4741E-04	4.98
4	0.1181E-07	6.01	0.1488E-05	4.99
5	0.1846E-09	6.00	0.4659E-07	5.00

We solve the 3D Poisson equation (1.1) on domain  $\Omega = (0, 1)^3$ , where an exact solution is chosen as

$$(5.2) \quad u(x, y, z) = 2^6(x - x^2)(y - y^2)(z - z^2).$$

In Table 3, we compute the 3D  $P_1$ – $P_5$  stabilizer-free virtual elements solutions for (5.2) on the cubic meshes shown in Figure 7. All virtual element solutions converge at rates of the optimal order in both  $L^2$  and  $H^1$  norms. In particular, we have one order superconvergence in  $H^1$  semi-norm for the  $P_1$  stabilizer-free virtual element solutions. Also, we have one order superconvergence in both  $H^1$  semi-norm and  $L^2$  for the  $P_2$  stabilizer-free virtual element solutions. But we do not have a theory for these superconvergences. It is surprising that the  $P_2$  solutions are more accurate than the  $P_3$  solutions in Table 3.

TABLE 2. The error profile for (5.1) on meshes shown in Figure 6.

Grid	$\ \Pi_h^\nabla u - u_h\ _0$	$O(h^r)$	$ \Pi_h^\nabla u - u_h _1$	$O(h^r)$
By the $P_1$ stabilizer-free virtual element.				
6	0.1142E-03	2.00	0.1255E-01	1.00
7	0.2855E-04	2.00	0.6273E-02	1.00
8	0.7137E-05	2.00	0.3136E-02	1.00
By the $P_2$ stabilizer-free virtual element.				
6	0.1011E-05	3.00	0.4338E-03	2.00
7	0.1265E-06	3.00	0.1085E-03	2.00
8	0.1581E-07	3.00	0.2712E-04	2.00
By the $P_3$ stabilizer-free virtual element.				
6	0.2132E-07	4.00	0.1081E-04	3.00
7	0.1332E-08	4.00	0.1351E-05	3.00
8	0.8329E-10	4.00	0.1689E-06	3.00
By the $P_4$ stabilizer-free virtual element.				
5	0.1200E-07	4.99	0.3029E-05	4.00
6	0.3756E-09	5.00	0.1894E-06	4.00
7	0.1175E-10	5.00	0.1185E-07	4.00
By the $P_5$ stabilizer-free virtual element.				
3	0.1177E-05	5.98	0.8909E-04	4.97
4	0.1842E-07	6.00	0.2800E-05	4.99
5	0.2895E-09	5.99	0.8776E-07	5.00

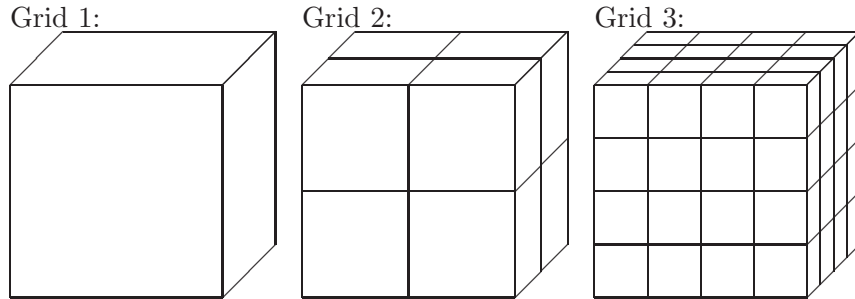


FIGURE 7. The first three grids for the computation in Table 3.

## 6. ETHICAL STATEMENT

### 6.1. Compliance with Ethical Standards.

TABLE 3. The error profile for (5.2) on cubic meshes shown in Figure 7.

Grid	$\ \Pi_h^\nabla u - u_h\ _0$	$O(h^r)$	$\ \Pi_h^\nabla u - u_h\ _1$	$O(h^r)$
By the 3D $P_1$ stabilizer-free virtual element.				
5	0.4944E-02	1.92	0.2780E-01	1.95
6	0.1254E-02	1.98	0.7011E-02	1.99
7	0.3145E-03	1.99	0.1757E-02	2.00
By the 3D $P_2$ stabilizer-free virtual element.				
5	0.1132E-04	3.89	0.1001E-02	2.85
6	0.7294E-06	3.96	0.1313E-03	2.93
7	0.4615E-07	3.98	0.1680E-04	2.97
By the 3D $P_3$ stabilizer-free virtual element.				
4	0.4149E-04	3.84	0.1569E-02	2.83
5	0.2688E-05	3.95	0.2053E-03	2.93
6	0.1703E-06	3.98	0.2618E-04	2.97
By the 3D $P_4$ stabilizer-free virtual element.				
4	0.7316E-06	4.94	0.4987E-04	3.94
5	0.2331E-07	4.97	0.3169E-05	3.98
6	0.7356E-09	4.99	0.1997E-06	3.99
By the 3D $P_5$ stabilizer-free virtual element.				
3	0.2986E-05	5.97	0.7301E-04	4.96
4	0.4707E-07	5.99	0.2318E-05	4.98
5	0.7386E-09	5.99	0.7304E-07	4.99

The submitted work is original and is not published elsewhere in any form or language.

## 6.2. Funding.

Yanping Lin is supported in part by HKSAR GRF 15302922 and polyu-CAS joint Lab.

Mo Mu is supported in part by Hong Kong RGC CERG HKUST16301218.

## 6.3. Conflict of Interest.

There is no potential conflict of interest .

## 6.4. Ethical approval.

This article does not contain any studies involving animals. This article does not contain any studies involving human participants.

### 6.5. Informed consent.

This research does not have any human participant.

### 6.6. Availability of supporting data.

This research does not use any external or author-collected data.

### 6.7. Authors' contributions.

All authors made equal contribution.

### 6.8. Acknowledgments.

None.

## REFERENCES

- [1] A. Al-Taweel, Y. Dong, S. Hussain and X. Wang, A weak Galerkin harmonic finite element method for Laplace equation, *Commun. Appl. Math. Comput.* 3 (2021), no. 3, 527–543.
- [2] A. Al-Twaeel, S. Hussian and X. Wang, A stabilizer free weak Galerkin finite element method for parabolic equation, *J. Comput. Appl. Math.*, 392 (2021), 113373.
- [3] A. Al-Twaeel, X. Wang, X. Ye and S. Zhang, A stabilizer free weak Galerkin element method with supercloseness of order two, *Numer. Methods Partial Differential Equations* 37 (2021), no. 2, 1012–1029.
- [4] L. Beirão da Veiga, F. Brezzi, A. Cangiani, G. Manzini, L. D. Marini and A. Russo, Basic principles of virtual element methods, *Math. Models Methods Appl. Sci.* 23 (2013) 199–214.
- [5] L. Beirão da Veiga, F. Brezzi, L. D. Marini and A. Russo,  $H(\text{div})$  and  $H(\text{curl})$ -conforming virtual element methods, *Numer. Math.* 133 (2016) 303–332.
- [6] S. Berrone, A. Borio, F. Marcon and G. Teora, A first-order stabilization-free virtual element method, *Appl. Math. Lett.* 142 (2023), Paper No. 108641, 6 pp.
- [7] S. Berrone, A. Borio and F. Marcon, Comparison of standard and stabilization free Virtual Elements on anisotropic elliptic problems, 2022, arXiv:2202.08571v1.
- [8] S. Berrone, A. Borio and F. Marcon, Lowest order stabilization free Virtual Element Method for the Poisson equation, 2023, arXiv:2103.16896v1.
- [9] S. Cao, L. Chen and R. Guo, A virtual finite element method for two-dimensional Maxwell interface problems with a background unfitted mesh, *Math. Models Methods Appl. Sci.* 31 (2021), no. 14, 2907–2936.
- [10] S. Cao, L. Chen and R. Guo, Immersed virtual element methods for electromagnetic interface problems in three dimensions, *Math. Models Methods Appl. Sci.* 33 (2023), no. 3, 455–503.
- [11] L. Chen, H. Wei and M. Wen, An interface-fitted mesh generator and virtual element methods for elliptic interface problems, *J. Comput. Phys.* 334 (2017), 327–348.
- [12] L. Chen and J. Huang, Some error analysis on virtual element methods, *Calcolo* 55 (2018), no. 1, Paper No. 5, 23 pp.
- [13] L. Chen and X. Huang, Nonconforming virtual element method for 2mth order partial differential equations in  $\mathbb{R}^n$ , *Math. Comp.* 89 (2020), no. 324, 1711–1744.
- [14] R.W. Clough and J.L. Tocher, Finite element stiffness matrices for analysis of plates in bending, in: *Proceedings of the Conference on Matrix Methods in Structural Mechanics*, Wright Patterson A.F.B. Ohio, 1965.
- [15] F. Feng, W. Han and J. Huang, Virtual element methods for elliptic variational inequalities of the second kind, *J. Sci. Comput.* 80 (2019), no. 1, 60–80.

- [16] F. Feng, J. Huang and Y. Yu, A non-consistent virtual element method for reaction diffusion equations, *East Asian J. Appl. Math.* 10 (2020), no. 4, 786–799.
- [17] Y. Feng, Y. Liu, R. Wang and S. Zhang, A conforming discontinuous Galerkin finite element method on rectangular partitions, *Electron. Res. Arch.* 29 (2021), no. 3, 2375–2389.
- [18] Y. Feng, Y. Liu, R. Wang and S. Zhang, A stabilizer-free weak Galerkin finite element method for the Stokes equations, *Adv. Appl. Math. Mech.* 14 (2022), no. 1, 181–201.
- [19] F. Gao, X. Ye and S. Zhang, A discontinuous Galerkin finite element method without interior penalty terms, *Adv. Appl. Math. Mech.* 14 (2022), no. 2, 299–314.
- [20] J. Huang and S. Lin, A C0P2 time-stepping virtual element method for linear wave equations on polygonal meshes, *Electron. Res. Arch.* 28 (2020), no. 2, 911–933.
- [21] J. Huang and Y. Yu, Some estimates for virtual element methods in three dimensions, *Comput. Methods Appl. Math.* 23 (2023), no. 1, 177–187.
- [22] J. Huang and Y. Yu, A medius error analysis for nonconforming virtual element methods for Poisson and biharmonic equations, *J. Comput. Appl. Math.* 386 (2021), Paper No. 113229, 20 pp.
- [23] L. Mu, X. Ye and S. Zhang, A stabilizer free, pressure robust and superconvergence weak Galerkin finite element method for the Stokes Equations on polytopal mesh, *SIAM J. Sci. Comput.*, 43 (2021), A2614–A2637.
- [24] L. Mu, X. Ye and S. Zhang, Development of pressure-robust discontinuous Galerkin finite element methods for the Stokes problem, *J. Sci. Comput.* 89 (2021), no. 1, Paper No. 26, 25 pp.
- [25] L. Mu, X. Ye and S. Zhang, A stabilizer free, pressure robust, and superconvergence weak Galerkin finite element method for the Stokes Equations on polytopal mesh, *SIAM J. Sci. Comput.* 43 (2021), no. 4, A2614–A2637.
- [26] L. Mu, X. Ye, S. Zhang and P. Zhu, A DG method for the Stokes equations on tensor product meshes with  $[P_k]^d - P_{k-1}$  element, *Communications on Applied Mathematics and Computation*, 2023, doi:10.1007/s42967-022-00243-9.
- [27] L. R. Scott and S. Zhang, Finite element interpolation of nonsmooth functions satisfying boundary conditions, *Math. Comp.* 54 (1990), no. 190, 483–493.
- [28] T. Sorokina and S. Zhang, Conforming and nonconforming harmonic finite elements, *Appl. Anal.* 99 (2020), no. 4, 569–584.
- [29] T. Sorokina and S. Zhang, Conforming harmonic finite elements on the Hsieh-Clough-Tocher split of a triangle, *Int. J. Numer. Anal. Model.* 17 (2020), no. 1, 54–67.
- [30] J. Wang, X. Ye and S. Zhang, Numerical investigation on weak Galerkin finite elements, *Int. J. Numer. Anal. Model.* 17 (2020) no. 4, 517–531.
- [31] J. Wang, X. Ye and S. Zhang, Weak Galerkin finite element methods with or without stabilizers, *Numer. Algorithms* 88 (2021), no. 3, 1361–1381.
- [32] J. Wang, X. Wang, X. Ye, S. Zhang and Peng Zhu, Two-order superconvergence for a weak Galerkin method on rectangular and cuboid grids, *Numer. Methods Partial Differential Equations* 39 (2023), no. 1, 744–758.
- [33] J. Wang, X. Wang, X. Ye, S. Zhang and Peng Zhu, On the superconvergence of a WG method for elliptic problem with variable coefficients, *Science China*, 2023, doi:10.1007/s11425-022-2097-8.
- [34] X. Xu and S. Zhang, A new divergence-free interpolation operator with applications to the Darcy-Stokes-Brinkman equations, *SIAM J. Sci. Comput.* 32 (2010), no. 2, 855–874.
- [35] X. Xu and S. Zhang, A family of stabilizer-free virtual elements on triangular meshes, 2023, arXiv:2309.09660.
- [36] X. Ye and S. Zhang, A conforming discontinuous Galerkin finite element method, *Int. J. Numer. Anal. Model.* 17 (2020) no. 1, 110–117.
- [37] X. Ye and S. Zhang, A conforming discontinuous Galerkin finite element method: Part II, *Int. J. Numer. Anal. Model.* 17 (2020), no. 2, 281–296.

- [38] X. Ye and S. Zhang, A stabilizer-free weak Galerkin finite element method on polytopal meshes. *J. Comput. Appl. Math.* 371 (2020), 112699, 9 pp.
- [39] X. Ye and S. Zhang, A Stabilizer Free Weak Galerkin Method for the Biharmonic Equation on Polytopal Meshes, *SIAM J. Numer. Anal.* 58 (2020), no. 5, 2572–2588.
- [40] X. Ye, S. Zhang and Y. Zhu, Stabilizer-free weak Galerkin methods for monotone quasilinear elliptic PDEs, *Results Appl. Math.* 8 (2020), Paper No. 100097, 10 pp.
- [41] X. Ye, S. Zhang and Y. Zhu, A conforming discontinuous Galerkin finite element method: Part III, *Int. J. Numer. Anal. Model.* 17 (2020), no. 6, 794–805.
- [42] X. Ye and S. Zhang, A stabilizer-free pressure-robust finite element method for the Stokes equations, *Adv. Comput. Math.* 47 (2021), no. 2, Paper No. 28, 17 pp.
- [43] X. Ye and S. Zhang, A stabilizer free weak Galerkin finite element method on polytopal mesh: Part II, *J. Comput. Appl. Math.* 394 (2021), Paper No. 113525, 11 pp.
- [44] X. Ye and S. Zhang, A stabilizer free weak Galerkin finite element method on polytopal mesh: Part III, *J. Comput. Appl. Math.* 394 (2021), Paper No. 113538, 9 pp.
- [45] X. Ye and S. Zhang, A new weak gradient for the stabilizer free weak Galerkin method with polynomial reduction, *Discrete Contin. Dyn. Syst. Ser. B* 26 (2021), no. 8, 4131–4145.
- [46] X. Ye and S. Zhang, A stabilizer free WG Method for the Stokes Equations with order two superconvergence on polytopal mesh, *Electron. Res. Arch.* 29 (2021), no. 6, 3609–3627.
- [47] X. Ye and S. Zhang, A numerical scheme with divergence free H-div triangular finite element for the Stokes equations, *Appl. Numer. Math.* 167 (2021), 211–217.
- [48] X. Ye and S. Zhang, A  $P_{k+2}$  polynomial lifting operator on polygons and polyhedrons, *Appl. Math. Lett.* 116 (2021), Paper No. 107033, 6 pp.
- [49] X. Ye and S. Zhang, A weak divergence CDG method for the biharmonic equation on triangular and tetrahedral meshes, *Appl. Numer. Math.* 178 (2022), 155–165.
- [50] X. Ye and S. Zhang, A  $C^0$ -conforming DG finite element method for biharmonic equations on triangle/tetrahedron, *J. Numer. Math.* 30 (2022), no. 3, 163–172.
- [51] X. Ye and S. Zhang, Achieving superconvergence by one-dimensional discontinuous finite elements: the CDG method, *East Asian J. Appl. Math.* 12 (2022), no. 4, 781–790.
- [52] X. Ye and S. Zhang, Order two superconvergence of the CDG method for the Stokes equations on triangle/tetrahedron, *Journal of Applied Analysis and Computation*, 12 (2022), no. 6, 2578–2592.
- [53] X. Ye and S. Zhang, Achieving superconvergence by one-dimensional discontinuous finite elements: weak Galerkin method, *East Asian J. Appl. Math.* 12 (2022), no. 3, 590–598.
- [54] X. Ye and S. Zhang, Constructing order two superconvergent WG finite elements on rectangular meshes, *Numer. Math. Theory Methods Appl.* 16 (2023), no. 1, 230–241.
- [55] X. Ye and S. Zhang, Order two superconvergence of the CDG finite elements on triangular and tetrahedral meshes, *CSIAM Trans. Appl. Math.* 4 (2023), no. 2, 256–274.
- [56] X. Ye and S. Zhang, Four-order superconvergent weak Galerkin methods for the biharmonic equation on triangular meshes, *Communications on Applied Mathematics and Computation*, Doi:10.1007/s42967-022-00201-5, 2023.
- [57] X. Ye and S. Zhang, Four-order superconvergent CDG finite elements for the biharmonic equation on triangular meshes, *J. Comput. Appl. Math.*, 2023, doi: 10.1016/j.cam.2023.115516.
- [58] S. Zhang, An optimal order multigrid method for biharmonic,  $C^1$  finite-element equations, *Numer. Math.* 56 (1989), 613–624.
- [59] S. Zhang, A new family of stable mixed finite elements for the 3D Stokes equations. *Math. Comp.* 74 (2005), no. 250, 543–554.

DEPARTMENT OF APPLIED MATHEMATICS, THE HONG KONG POLYTECHNIC UNIVERSITY, HUNG HOM, HONG KONG

*Email address:* [yanping.lin@polyu.edu.hk](mailto:yanping.lin@polyu.edu.hk)

DEPARTMENT OF MATHEMATICS, HONG KONG UNIVERSITY OF SCIENCE AND TECHNOLOGY, CLEAR WATER BAY, KOWLOON, HONGKONG, CHINA

*Email address:* [mamu@ust.hk](mailto:mamu@ust.hk)

DEPARTMENT OF MATHEMATICAL SCIENCES, UNIVERSITY OF DELAWARE, NEWARK, DE 19716, USA.

*Email address:* [szhang@udel.edu](mailto:szhang@udel.edu)